International Journal of Power Electronics and Drive System (IJPEDS)
Vol. 5, No. 4, April 2015, pp. 453~463
ISSN: 2088-8694

Three-Level DTC Based on Fuzzy Logic and Neural Network of Sensorless DSSM Using Extende Kalman Filter

Elakhdar Benyoussef[*], Abdelkader Meroufel[*], Said Barkat[**]
[*]Faculty of Science and Engineering, Department of Electrical Engineering, University of Djilali Liabes, Sidi Bel Abbes 22000, BP 89 Algeria, Intelligent Control Electronic Power System laboratory (I.C.E.P.S)
[**]Faculty of Technology, Department of Electrical Engineering, University of M'sila, Ichbilia Street, M'sila 28000, BP 166 Algeria

Article Info

Article history:

Received Nov 7, 2014
Revised Jan 15, 2015
Accepted Jan 28, 2015

Keyword:

Direct Torque Control
Double Star
Extended Kalman Filter
Fuzzy Logic Control
Multilevel Inverter
Neural Network
Synchronous Machine

ABSTRACT

This paper presents a direct torque control is applied for salient-pole double star synchronous machine without mechanical speed and stator flux linkage sensors. The estimation is performed using the extended Kalman filter known by it is ability to process noisy discrete measurements. Two control approaches using fuzzy logic DTC, and neural network DTC are proposed and compared. The validity of the proposed controls scheme is verified by simulation tests of a double star synchronous machine. The stator flux, torque, and speed are determined and compared in the above techniques. Simulation results presented in this paper highlight the improvements produced by the proposed control method based on the extended Kalman filter under various operation conditions.

Corresponding Author:

Elakhdar Benyoussef,
Department of Electrical Engineering,
Djilali Liabes University,
Sidi Bel Abbes 22000, BP 89 Algeria.
Email: lakhdarbenyoussef@yahoo.com

1. INTRODUCTION

A multiphase drive has more than three phases in the stator and the same number of inverter legs is in the inverter side. The main advantages of multiphase drives over conventional three-phase drives include increasing the inverter output power, reducing the amplitude of torque ripple and lowering the DC link current harmonics. Furthermore, the multiphase drive system is able to improve the reliability. Indeed, the motor can start and run since the loss of one or many phases [1]. Last two decades, the multiphase drive systems have been used in many applications, such as traction, electric/hybrid vehicles, and ship propulsion [2].

In multiphase machine drive systems, more than threephase windings are implemented in the same stator of the electric machine. One common example of such structure is the double star synchronous motor (DSSM). This motor has two sets of three-phase windings spatially phase shifted by 30 electrical degrees and each set of three-phase stator windings is fed by a three-phase voltage source inverter [3].

The feeding of the DSSM is generally assured by two twolevel inverters. However, for the high power; multilevel inverters are often required. Since the advantages of multilevel inverters and multiphase machines complement each other, it appears to be logical to try to combine them by realizing a multilevel multiphase drive [4]. In the other hand, multilevel inverter fed electric machine systems are considered as a promising approach in achieving high power/high voltage ratings. Moreover, multilevel inverters have the

advantages of overcoming voltage limit capability of semiconductor switches, and improving 2 harmonic profiles of output waveforms [5]. The output voltage waveform approaches a sine wave, thus having practically no common-mode voltage and no voltage surge to the motor windings. Furthermore, the reduction in *dv*/*dt* can prevent motor windings and bearings from failure.

In the other hand, the multilevel direct torque control (DTC) of electrical drives has become an attracting topic in research and academic community over the past decade. Like an every control method has some advantages and disadvantages, DTC method has too. Some of the advantages are presented in [6]. The basic disadvantages of DTC scheme using hysteresis controllers are the variable switching frequency, the current and torque ripple. In the aim to improve the performance of the electrical drives based on traditional DTC, fuzzy logic direct torque control (FLDTC) and artificial neural network direct torque control (DTC-ANN) attracts more and more the attention of many scientists [7], [8]. This paper is devoted to FLDTC and DTC-ANN of sensorless DSSM using extended Kalman filter fed by two three-level diode clamped inverter (DCI).

In this context, several speed observers have been suggested in literature, such as sliding mode observer [9], adaptive observer, model reference adaptive system, and Extende Kalman filter [10]. Kalman filter is a stochastic state observer where nonlinear equations are linearized in every sampling period. It has the advantage of providing both flux and speed estimates, and thus avoids limitations of the open loop pure integration method.

The present paper structure is as follows. Firstly, the model of the DSSM is presented in the second section. In the third section, the three-level inverter modeling is described. In the fourth section, the FLDTC strategy is applied to get decoupled control of the stator flux and electromagnetic torque. Next, a brief introduction on the EKF algorithm is presented in the fifth section. The sixth section introduces the DTC-ANN approach. The seventh section is devoted to the comparative study between three-level FLDTC and three-level DTC-ANN of sensorless DSSM. Finally, conclusions are drawn in the last section.

2. MODELING OF THE DOUBLE STAR SYNCHRONOUS MACHINE

The stator voltages equations are given by:

$$\begin{cases} v_{s1} = R_s i_{s1} + \dfrac{d\phi_{s1}}{dt} \\ v_{s2} = R_s i_{s2} + \dfrac{d\phi_{s2}}{dt} \end{cases} \quad (1)$$

With

v_{s1}, v_{s2} : Stator voltages.

i_{s1}, i_{s2} : Stator currents.

ϕ_{s1}, ϕ_{s2} : Stator flux.

The rotor voltage equation is given by:

$$v_f = R_f i_f + \frac{d\phi_f}{dt} \quad (2)$$

With:

ϕ_f : Flux of rotor excitation.

v_f, i_f : Voltage and current of rotor excitation.

The transformation of the system six phases to the system (α, β) is given by:

$$\begin{bmatrix} X_\alpha & X_\beta \end{bmatrix} = [A] \begin{bmatrix} X_{s1} & X_{s2} \end{bmatrix} \quad (3)$$

Where:

X_{s1} and X_{s2} can represent the stator currents, stator flux, and stator voltages.

The transformation matrix *A* is given by:

$$[A]=\frac{1}{\sqrt{3}}\begin{pmatrix} 1 & -\frac{1}{2} & -\frac{1}{2} & \frac{\sqrt{3}}{2} & -\frac{\sqrt{3}}{2} & 0 \\ 0 & \frac{\sqrt{3}}{2} & -\frac{\sqrt{3}}{2} & \frac{1}{2} & \frac{1}{2} & -1 \\ 1 & -\frac{1}{2} & -\frac{1}{2} & -\frac{\sqrt{3}}{2} & \frac{\sqrt{3}}{2} & 0 \\ 0 & -\frac{\sqrt{3}}{2} & \frac{\sqrt{3}}{2} & \frac{1}{2} & \frac{1}{2} & -1 \\ 1 & 1 & 1 & 0 & 0 & 0 \\ 0 & 0 & 0 & 1 & 1 & 1 \end{pmatrix} \quad (4)$$

To express the stator equations in the same reference frame, the following rotation transformation is adopted.

$$P(\theta)=\begin{pmatrix} \cos(\theta) & \sin(\theta) \\ -\sin(\theta) & \cos(\theta) \end{pmatrix} \quad (5)$$

With: θ is the rotor position.

With this transformation, the components of the α-β plane can be expressed in the *d*-*q* plane as:

The electrical equations

$$\begin{cases} v_d = R_s i_d + \dfrac{d\phi_d}{dt} - \omega\phi_q \\ v_q = R_s i_q + \dfrac{d\phi_q}{dt} + \omega\phi_d \end{cases} \quad (6)$$

Where:

v_d, v_q : Stator voltages *dq* components.

i_d, i_q : Stator currents *dq* components.

ϕ_d, ϕ_q : Stator flux *dq* components.

The flux equations

$$\begin{cases} \phi_d = L_d i_d + M_{fd} i_f \\ \phi_q = L_q i_q \\ \phi_f = L_f i_f + M_{fd} i_d \end{cases} \quad (7)$$

The mechanical equation

$$J\frac{d\Omega}{dt} = T_{em} - T_L - f\,\Omega \quad (8)$$

With:

T_{em}, T_L : Electromagnetic and load torque.

Ω : Rotor speed.

The electromagnetic torque

$$T_{em} = p\left(\phi_d i_q - \phi_q i_d\right) \quad (9)$$

3. MODELING OF THE THREE-LEVEL INVERTER

Figure 1 shows the circuit of a three-level diode clamped inverter and the switching states of each leg of the inverter. Each leg is composed of two upper and lower switches with anti-parallel diodes. Two series DC-link capacitors split the DC-bus voltage in half, and six clamping diodes confine the voltage across

the switches within the voltage of the capacitors, each leg of the inverter can have three possible switching states; 2, 1 or 0 [11].

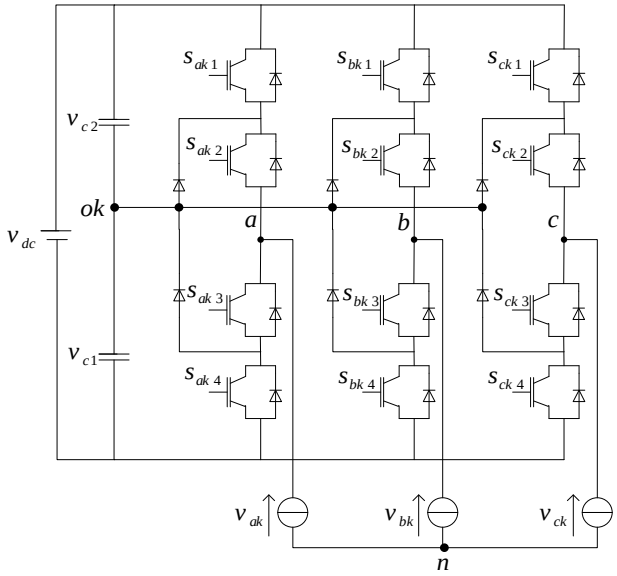

Figure 1. Schematic diagram of a three-level inverter (k=1 for first inverter and k=2 for second inverter)

The representation of the space voltage vectors of a three-level inverter for all switching states is given by Figure 2. According to the magnitude of the voltage vectors, the voltage vectors can be partitioned into four groups: the zero voltage vectors v_0, the large voltage vectors (v_{1L}, v_{3L}, v_{5L}, v_{7L}, v_{9L}, v_{11L}), the middle voltage vectors (v_{2L}, v_{4L}, v_{6L}, v_{8L}, v_{10L}, v_{12L}), and the small voltage vectors (v_{1S}, v_{2S}, v_{3S}, v_{4S}, v_{5S}, v_{6S}).

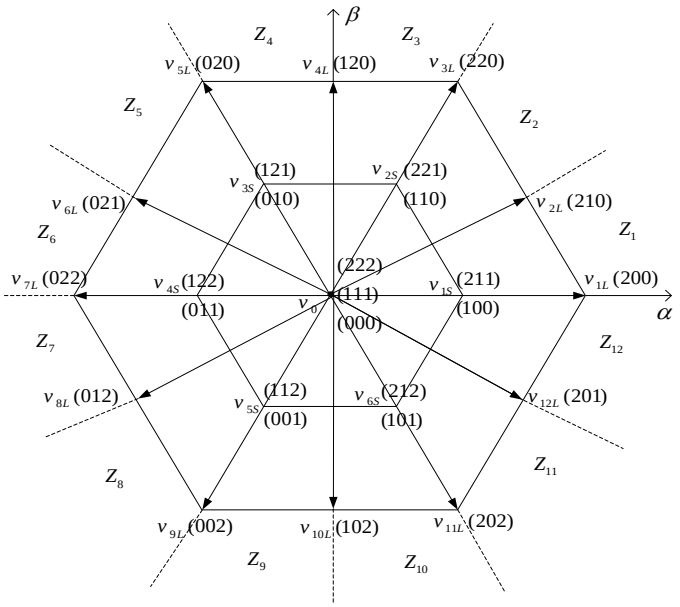

Figure 2. Space vector diagram of three-level inverter

4. DIRECT TORQUE CONTROL BASED ON FUZZY LOGIC STRATEGY

The principle of fuzzy logic direct torque control is similar to traditional DTC. However, the hysteresis controllers are replaced by fuzzy controller and the output vector of the fuzzy controller is led to a switching table to decide which vector should be applied. This method based on fuzzy classification has the advantage of simplicity and easy implementation [8].

The components of stator flux can be estimated by:

$$\begin{cases} \hat{\phi}_\alpha(t) = \int_0^t (\hat{v}_\alpha - R_s i_\alpha)\, d\tau + \hat{\phi}_\alpha(0) \\ \hat{\phi}_\beta(t) = \int_0^t (\hat{v}_\beta - R_s i_\beta)\, d\tau + \hat{\phi}_\beta(0) \end{cases} \quad (10)$$

The stator flux amplitude is given by:

$$\left|\hat{\phi}_s\right| = \sqrt{\hat{\phi}_\alpha^2 + \hat{\phi}_\beta^2} \quad (11)$$

The stator flux angle is calculated by:

$$\hat{\theta}_s = \tan 2^{-1}\left(\frac{\hat{\phi}_\beta}{\hat{\phi}_\alpha}\right) \quad (12)$$

Electromagnetic torque equation is given by:

$$\hat{T}_{em} = p\left(\hat{\phi}_\alpha i_\beta - \hat{\phi}_\beta i_\alpha\right) \quad (13)$$

The fuzzy controller is designed to have three fuzzy state variables and one control variable for achieving constant torque and flux control. The first variable $(E_\phi = \hat{\phi}_s - \phi_s^*)$ is the difference between the command stator flux ϕ_s^* and the estimated stator flux magnitude $\hat{\phi}_s$. The second variable $(E_T = \hat{T}_{em} - T_{em}^*)$ is the difference between the command electric torque T_{em}^* and estimated electric torque $\hat{T}_{em}$. The third fuzzy state variable is the stator flux phase $(\hat{\theta}_s)$. Figure 3 gives the membership functions for input variables E_ϕ, E_T and $\hat{\theta}_s$.

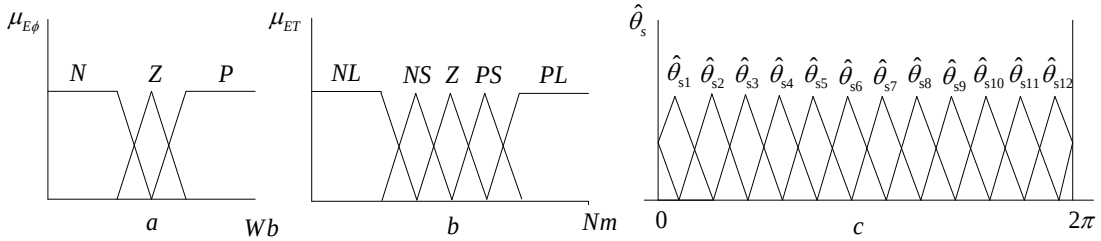

Figure 3. Membership functions of input variables: a) Stator flux error, b) Torque error, c) Stator flux angle

The switching tables of the proposed three-level FLDTC are used to select the best output voltage depending on the position of the stator flux and desired action on the torque and stator flux. The optimal voltage vector selection, for controlling both the amplitude and rotating direction of the stator flux, is indicated in Table 1, 2. The linguistic terms used for stator flux error are N (negative), Z (zero), and P (positive). For the torque error, the terms used are NL (negative large), NS (negative small), ZE (zero), PS (positive small), and PL (positive large).

Table 1. Rules of fuzzy control for first star

$\hat{\theta}_{s1}$				$\hat{\theta}_{s2}$				$\hat{\theta}_{s3}$			
E_T E_ϕ	P	Z	N	E_T E_ϕ	P	Z	N	E_T E_ϕ	P	Z	N
PL	v_{3L}	v_{2S}	v_{5L}	PL	v_{3L}	v_{2S}	v_{5L}	PL	v_{5L}	v_{3S}	v_{7L}
PS	v_{2L}	v_{2S}	v_{4L}	PS	v_{4L}	v_{3S}	v_{6L}	PS	v_{4L}	v_{3S}	v_{6L}
ZE	0	0	0	ZE	0	0	0	ZE	0	0	0
NS	v_{12L}	0	v_{10L}	NS	v_{12L}	0	v_{10L}	NS	v_{2L}	0	v_{12L}
NL	v_{11L}	v_{5S}	v_{9L}	NL	v_{1L}	v_{6S}	v_{11L}	NL	v_{1L}	v_{6S}	v_{11L}
$\hat{\theta}_{s4}$				$\hat{\theta}_{s5}$				$\hat{\theta}_{s6}$			
E_T E_ϕ	P	Z	N	E_T E_ϕ	P	Z	N	E_T E_ϕ	P	Z	N
PL	v_{5L}	v_{3S}	v_{7L}	PL	v_{7L}	v_{4S}	v_{9L}	PL	v_{7L}	v_{4S}	v_{9L}
PS	v_{6L}	v_{4S}	v_{8L}	PS	v_{6L}	v_{4S}	v_{8L}	PS	v_{8L}	v_{5S}	v_{10L}
ZE	0	0	0	ZE	0	0	0	ZE	0	0	0
NS	v_{2L}	0	v_{12L}	NS	v_{4L}	0	v_{2L}	NS	v_{4L}	0	v_{2L}
NL	v_{10L}	v_{1S}	v_{1L}	NL	v_{3L}	v_{1S}	v_{1L}	NL	v_{5L}	v_{2S}	v_{3L}
$\hat{\theta}_{s7}$				$\hat{\theta}_{s8}$				$\hat{\theta}_{s9}$			
E_T E_ϕ	P	Z	N	E_T E_ϕ	P	Z	N	E_T E_ϕ	P	Z	N
PL	v_{9L}	v_{5S}	v_{11L}	PL	v_{9L}	v_{5S}	v_{11L}	PL	v_{11L}	v_{6S}	v_{1L}
PS	v_{8L}	v_{5S}	v_{10L}	PS	v_{10L}	v_{6S}	v_{12L}	PS	v_{10L}	v_{6S}	v_{12L}
ZE	0	0	0	ZE	0	0	0	ZE	0	0	0
NS	v_{6L}	0	v_{4L}	NS	v_{6L}	0	v_{4L}	NS	v_{8L}	0	v_{6L}
NL	v_{5L}	v_{2S}	v_{3L}	NL	v_{7L}	v_{3S}	v_{5L}	NL	v_{7L}	v_{3S}	v_{5L}
$\hat{\theta}_{s10}$				$\hat{\theta}_{s11}$				$\hat{\theta}_{s12}$			
E_T E_ϕ	P	Z	N	E_T E_ϕ	P	Z	N	E_T E_ϕ	P	Z	N
PL	v_{11L}	v_{6S}	v_{1L}	PL	v_{1L}	v_{1S}	v_{3L}	PL	v_{1L}	v_{1S}	v_{3L}
PS	v_{12L}	v_{1S}	v_{2L}	PS	v_{12L}	v_{1S}	v_{2L}	PS	v_{2L}	v_{2S}	v_{4L}
ZE	0	0	0	ZE	0	0	0	ZE	0	0	0
NS	v_{8L}	0	v_{6L}	NS	v_{10L}	0	v_{8L}	NS	v_{10L}	0	v_{8L}
NL	v_{9L}	v_{4S}	v_{7L}	NL	v_{9L}	v_{4S}	v_{7L}	NL	v_{11L}	v_{5S}	v_{9L}

Table 2. Rules of fuzzy control for second star

*star*1	$\hat{\theta}_{s12}$	$\hat{\theta}_{s1}$	$\hat{\theta}_{s2}$	$\hat{\theta}_{s3}$	$\hat{\theta}_{s4}$	$\hat{\theta}_{s5}$	$\hat{\theta}_{s6}$	$\hat{\theta}_{s7}$	$\hat{\theta}_{s8}$	$\hat{\theta}_{s9}$	$\hat{\theta}_{s10}$	$\hat{\theta}_{s11}$
*star*2	$\hat{\theta}_{s1}$	$\hat{\theta}_{s2}$	$\hat{\theta}_{s3}$	$\hat{\theta}_{s4}$	$\hat{\theta}_{s5}$	$\hat{\theta}_{s6}$	$\hat{\theta}_{s7}$	$\hat{\theta}_{s8}$	$\hat{\theta}_{s9}$	$\hat{\theta}_{s10}$	$\hat{\theta}_{s11}$	$\hat{\theta}_{s12}$

5. SPEED ESTIMATION BASED ON EXTENDED KALMAN FILTER

Kalman filter is a state observer that establishes the best approximation by minimization of the square error for the state variables of a system, subjected at both its input and output to random disturbances. If the dynamic system of which the state is being observed is nonlinear, then the Kalman filter is called an extended one (EKF) [10]. The development of the Kalman filter is closely linked to the stochastic systems. The linear stochastic systems are described by:

$$\begin{cases} \dot{x}(t) = Ax(t) + Bu(t) + w(t),\ x(t_o) = x_o \\ y(t) = Cx(t) + v(t) \end{cases} \tag{14}$$

Where: *w* and *v* are the system and measurement noise.

Estimation of an error covariance matrix:

$$P^{-}(k+1) = A_d P(k) A_d^T + Q \tag{15}$$

Computations of a Kalman filter gain:

$$K(k+1) = P^{-}(k+1) C^T \left(C P^{-}(k+1) C^T + R \right)^{-1} \tag{16}$$

Update of an error covariance matrix:

$$P(k+1) = \left(I - K(k+1) C \right) P^{-}(k+1) \tag{17}$$

State estimation:

$$\hat{x}(k+1) = \hat{x}(k) + K(k+1) \left(y(k+1) - C.\hat{x}(k+1) \right) \tag{18}$$

Where:

$P^{-}(k+1)$: is a priori error covariance matrix Q and R respectively.

The extended Kalman filter implementation for a DSSM requires three basic steps:
a) Continuous DSSM model
b) Discretization of the DSSM model
c) Simulation

5.1. Continuous DSSM Model

The model of DSSM in the α-β reference can be written in the following from:

$$\begin{cases} \dot{x}(t) = Ax(t) + Bu(t) \\ y(t) = Cx(t) \end{cases} \tag{19}$$

With:

$$x(t) = \begin{bmatrix} i_\alpha & i_\beta & \phi_\alpha & \phi_\beta & \Omega & \theta \end{bmatrix}$$

$$y = \begin{bmatrix} i_\alpha & i_\beta \end{bmatrix},\ u = \begin{bmatrix} v_\alpha & v_\beta \end{bmatrix}$$

$$A = \begin{bmatrix} -R_s & -p\Omega L_q & 0 & p\Omega & 0 & 0 \\ p\Omega L_q & -R_s & -p\Omega & 0 & 0 & 0 \\ -R_s & 0 & 0 & 0 & 0 & 0 \\ 0 & -R_s & 0 & 0 & 0 & 0 \\ -p\phi_\beta / J & p\phi_\alpha / J & 0 & 0 & -f/J & 0 \\ 0 & 0 & 0 & 0 & p & 0 \end{bmatrix},\ B = \begin{bmatrix} 1/L_q & 0 & 0 \\ 0 & 1/L_q & 0 \\ 1 & 0 & 0 \\ 0 & 1 & 0 \\ 0 & 0 & -f/J \\ 0 & 0 & 0 \end{bmatrix}$$

With:

$$\begin{cases} \phi_\alpha = L_q i_\alpha + \phi_f \cos(\theta) \\ \phi_\beta = L_q i_\beta + \phi_f \sin(\theta) \end{cases}$$

5.2. Discretization of the DSSM Model

The corresponding discrete time model is given by:

$$\begin{cases} x_{(k+1)} = A_d x_{(k)} + B_d u_{(k)} \\ y_{(k+1)} = C_d x_{(k)} \end{cases} \quad (20)$$

The conversion is done by the following approximation:

$$\begin{cases} A_d = e^{At} = I + AT_s \\ B_d = \int_0^t e^{A\xi} Bd\xi = BT_s \\ C_d = C \end{cases} \quad (21)$$

5.3. Simulation

Based on the previous elements, the EKF can now be built and applied to the DSSM. By derivation of the vector function in relation to the state vector, matrix A_d, B_d and C_d are given by:

$$A_d = \begin{bmatrix} 1-T_s R_s/L_q & -T_s p\Omega L_q & 0 & T_s p\Omega & 0 & 0 \\ T_s p\Omega L_q & 1-T_s R_s/L_q & -T_s p\Omega & 0 & 0 & 0 \\ -T_s R_s & 0 & 0 & 0 & 0 & 0 \\ 0 & -T_s R_s & 1 & 0 & 0 & 0 \\ -T_s p\phi_\beta/J & T_s p\phi_\alpha/J & 0 & 1 & -T_s f/J & 0 \\ 0 & 0 & 0 & 0 & T_s p & 1 \end{bmatrix}, \; B_d = \begin{bmatrix} T_s/L_q & 0 & 0 \\ 0 & T_s/L_q & 0 \\ T_s & 0 & 0 \\ 0 & T_s & 0 \\ 0 & 0 & -T_s f/J \\ 0 & 0 & 0 \end{bmatrix}, \; C_d = \begin{bmatrix} 1 & 0 & 0 & 0 & 0 \\ 0 & 1 & 0 & 0 & 0 \end{bmatrix}$$

The structure of DTC based on fuzzy logic control of DSSM is shown in Figure 4.

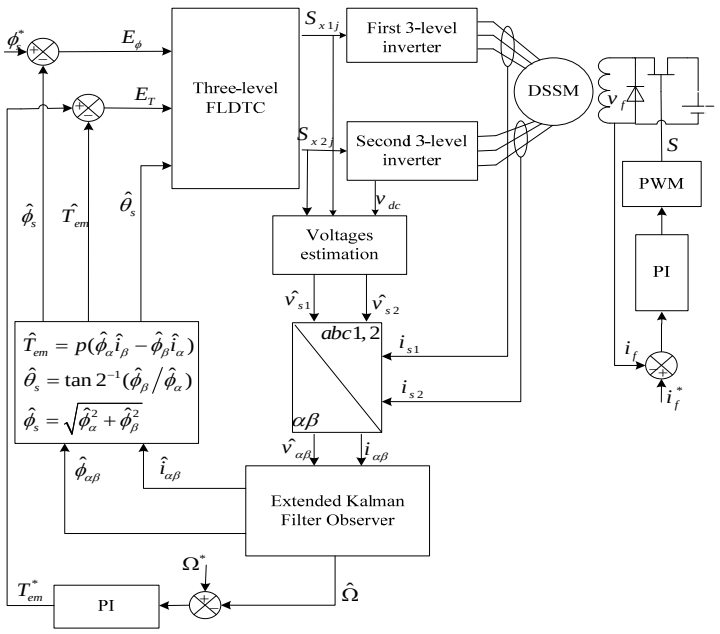

Figure 4. Three-level FLDTC scheme for sensorless DSSM (with *j=1, 2, 3* or *4*)

6. DIRECT TORQUE CONTROL BASED ON NEURAL NETWORK STRATEGY

The ANN has many models; but the usual model is the multilayer feed forward net work using the error back propagation algorithm [9]. Such a neural network contains three layers: input layers, hidden layers and output layers (Figure 5). Each layer is composed of several neurons. The number of the neurons in the input and output layers depends on the number of the selected input and output variables. The number of hidden layers and the number of neurons in each depend on the desired degree of accuracy.

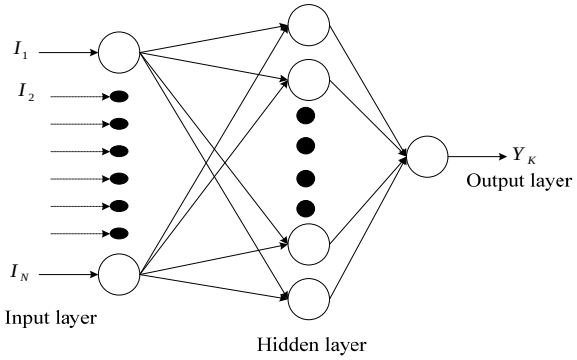

Figure 5. Architecture of Multilayer Neural Network

The structure of the neural network to perform the DTC applied to DSSM satisfactorily was a neural network with 3 linear input nodes, 12 neurons in the hidden layer, and 6 neurons in the output layer, as shown in Figure 6.

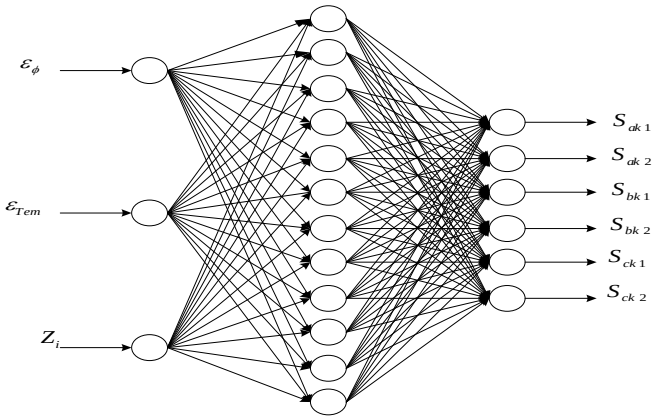

Figure 6. Neural network structure for three-level DTC

The general structure of the DSSM with DTC-ANN using a three-level inverter in each star is represented by Figure 7.

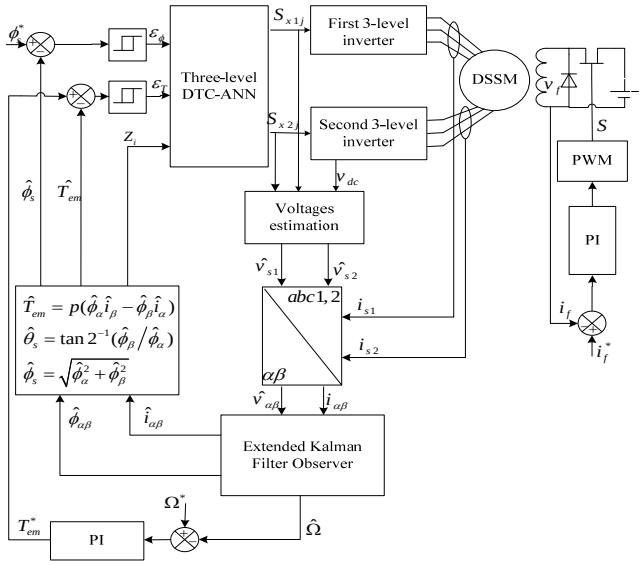

Figure 7. Three-level DTC-ANN scheme for sensorless DSSM (with *j=1, 2, 3* or *4*)

7. SIMULATION RESULTS

The proposed controls based on EKF observer are tested by some numerical simulations to verify its effectiveness in the steady-state and dynamic. Parameters of EKF are chosen as following to ensure filter not divergent.

$$[Q]=\begin{bmatrix} 100 & 0 & 0 & 0 & 0 & 0 \\ 0 & 100 & 0 & 0 & 0 & 0 \\ 0_s & 0 & 0.1 & 0 & 0 & 0 \\ 0 & 0 & 0 & 0.1 & 0 & 0 \\ 0 & 0 & 0 & 0 & 0.1 & 0 \\ 0 & 0 & 0 & 0 & 0 & 0.1 \end{bmatrix}, \quad [P]=\begin{bmatrix} 0.1 & 0 & 0 & 0 & 0 & 0 \\ 0 & 0.1 & 0 & 0 & 0 & 0 \\ 0 & 0 & 10^{-5} & 0 & 0 & 0 \\ 0 & 0 & 0 & 10^{-5} & 0 & 0 \\ 0 & 0 & 0 & 0 & 10^{-5} & 0 \\ 0 & 0 & 0 & 0 & 0 & 0.1 \end{bmatrix}, \quad [R]=\begin{bmatrix} 0.12 & 0 \\ 0 & 0.12 \end{bmatrix}$$

The simulation results of three-level DTC-ANN of sensorless DSSM are compared with three-level FLDTC. For this end, the controls system was tested under deferent operating conditions such as sudden change of load torque and step change in reference speed.

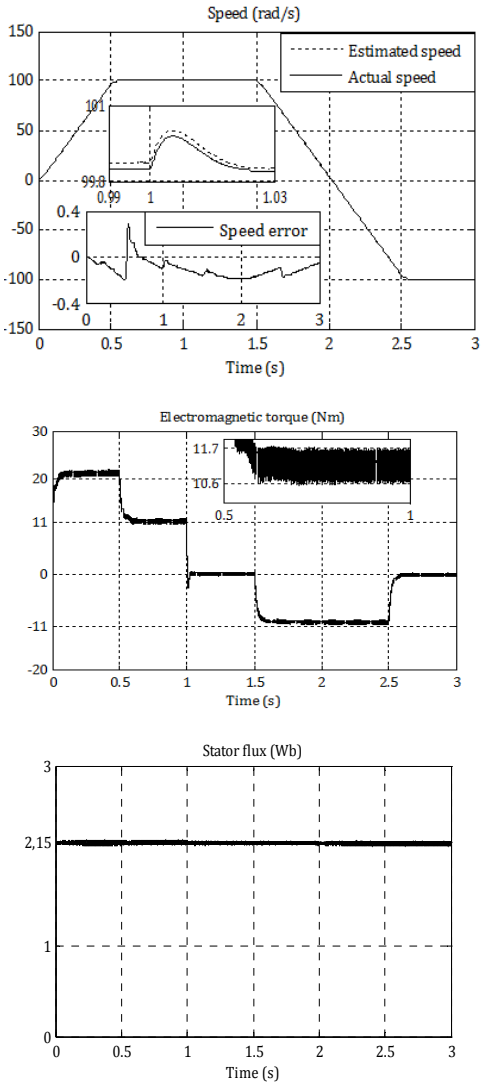

Figure 8. Dynamic responses of three-level FLDTC for sensorless DSSM

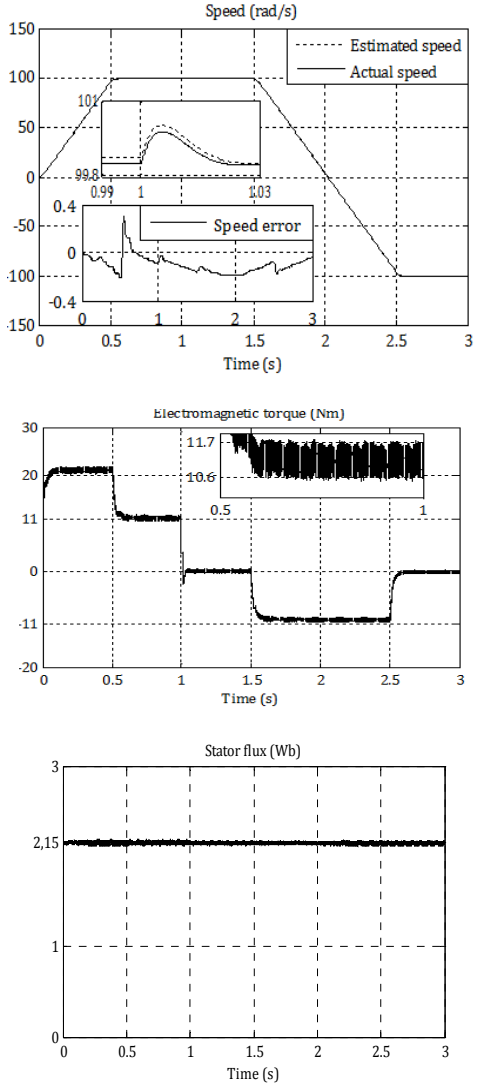

Figure 9. Dynamic responses of three-level DTC-ANN for sensorless DSSM

The obtained results are presented in Figure 8 for the three-level FLDTC and Figure 9 for the three-level DTC-ANN of DSSM without speed sensor. The DSSM is accelerating from standstill to reference speed *100* rad/s. The system is started with full load torque (T_L=*11* N.m). Afterwards, a step variation on the load torque (T_L=*0* N.m) is applied at time *t=1*s. And then a sudden reversion in the speed command from *100* rad/s to -*100* rad/s was introduced at *1.5* s.

Figure 8 and 9 depict that the speed response is merged with the reference one and the flux is constant equal to its rated value. As it can be seen, the employment of three-level DTC-ANN without speed sensor permits to obtain the same dynamic performances as those obtained with a three-level FLDTC without speed sensor. Indeed the observed and actual speed responses are closed to their reference without any overshoot and steady-state error.

The obtained results shown that the three-level DTC-ANN sensorless DSSM ensures good decoupling between stator flux linkage and electromagnetic torque. Also, it can decrease the torque ripples in comparison to the three-level FLDTC sensorless DSSM.

8. Conclusion

In this paper, a direct torque control based on artificial neural network and fuzzy logic methods applied of sensorless double star synchronous machine using extended Kalman filter is presented. It is pointed out that the robustness of the controlled double star synchronous machine drive against speed and load torque variations is guaranteed. Furthermore, the DTC-ANN control scheme decreases considerably the electromagnetic torque ripples and assures good speed tracking without overshoot. The decoupling between the stator flux and the electromagnetic torque is maintained, confirming the good dynamic performances of the developed multiphase drive system. Also, the robustness of the observer, against speed and load variations confirms the good dynamic performances of the developed sensorless multiphase drive.

References

[1] L Nezli, M Mahmoudi. Vector Control with Optimal Torque of a Salient–Pole Double Star Synchronous Machine Supplied by Three–Level Inverters. *Journal of Electrical Engineering*. 2010; 61(5): 257-263.
[2] A Matyas, A BiroK, D Fodorean. Multi-phase Synchronous Motor Solution for Steering Applications. *Progress in Electromagnetic Research*. 2012; 131: 63-80.
[3] S Kallio, M Andriollo, A Tortella, J Karttunen. Decoupled d–q Model of Double-Star Interior-Permanent-Magnet Synchronous Machines. *IEEE Transactions on Industrial Electronics*. 2013; 60(6): 2486-2494.
[4] E Benyoussef, A Meroufel, S Barkat. Multilevel Direct Torque Balancing Control of Double Star Synchronous Machine. *Journal of Electrical Engineering*. 2014; 1-11.
[5] B Singh, N Mittal, D Verma, D Singh, S Singh, R Dixit, M Singh, A Baranwal. Multi-Level Inverter: a Literature Survey on Topologies and Control Strategies. *International Journal of Reviews in Computing*. 2012; 10: 1-16.
[6] B Naas, L Nezli, M Mahmoudi, M Elbar. Direct Torque Control Based Three-Level Inverter Fed Double Star Permanent Magnet Synchronous Machine. *Energy Procedia*. 2012; 18: 521-530.
[7] F Kadri, S Drid, D Djarah, F Djeffal. Direct Torque Control of Induction Motor Fed by Three Phase PWM Inverter Using Fuzzy Logic and Neural Network. *Sixth International Conference on Electrical Engineering*. 2010; 12-16.
[8] A Tessarolo, D Giulivo. Direct Torque Control of Induction Motors with Fuzzy Logic Controller. *International Symposium on Power Electronics, Electrical Drives, Automation and Motion*. 2010; 845-852.
[9] X Zhuang, M Rahman. Comparison of a Sliding Observer and a Kalman Filter for Direct Torque Controlled IPM Synchronous Motor Drives. *IEEE, Transactions on Industrial Electronics*. 2012; 59(11): 4179-4188.
[10] M Merzoug, H Benalla, H Naceri. Speed Estimation Using Extended Filter Kalman for the Direct Torque Controlled Permanent Magnet Synchronous Motor (PMSM). *IEEE, International Conference on Computer and Electrical Engineering*, Dubai. 2009; 124-127.
[11] H Kalpesh, P Agarwal. Space Vector Modulation with DC Link Voltage Balancing Control for Three Level Inverters. *International Journal of Recent Trends in Engineering*. 2009; 1(3): 229-233.